Eco-evolutionary dynamics and collective migration: implications for salmon metapopulation robustness

Justin D. Yeakel[1,2,*], Jean P. Gibert[1], Peter A. H. Westley[3], & Jonathan W. Moore[4]

[1]School of Natural Sciences, University of California, Merced, Merced CA, USA

[2]The Santa Fe Institute, Santa Fe NM, USA

[3]College of Fisheries and Ocean Sciences, University of Alaska, Fairbanks, Fairbanks AK, USA

[4]Earth$_2$Oceans Research Group, Simon Fraser University, Burnaby BC, Canada

[*]To whom correspondence should be addressed: jdyeakel@gmail.com

The spatial dispersal of individuals is known to play an important role in the dynamics of populations, and is central to metapopulation theory. At the same time, local adaptation to environmental conditions creates a geographic mosaic of evolutionary forces, where the combined drivers of selection and gene flow interact. Although the dispersal of individuals from donor to recipient populations provides connections within the metapopulation, promoting demographic and evolutionary rescue, it may also introduce maladapted individuals into habitats host to different environmental conditions, potentially lowering the fitness of the recipient population. Here we explore a minimal model of the eco-evolutionary dynamics between two populations connected by dispersal, where the productivity of each is defined by a trait complex that is subject to local selection. Although general in nature, our model is inspired by salmon metapopulations, where dispersal between populations is defined in terms of the *straying rate*, which has been shown to be density dependent, and recently proposed to be shaped by social interactions consistent with collective movement. The results of our model reveal that increased straying between evolving populations leads to alternative stable states, which has large and nonlinear effects on two measures of metapopulation robustness: the portfolio effect and the time to recovery following an induced disturbance. We show that intermediate levels of straying result in large gains in robustness, and that increased habitat heterogeneity promotes robustness when straying rates are low, and erodes robustness when straying rates are high. Finally, we show that density-dependent straying promotes robustness, particularly when the aggregate biomass is low and straying is correspondingly high, and this has important ramifications for the conservation of salmon metapopulations facing both natural and anthropogenic disturbances.

Salmon metapopulations, Straying, Dispersal, Eco-evolutionary dynamics, Alternative stable states

Media Summary The rate at which individuals move within a metapopulation has large impacts on extinction risk. Among migratory species such as salmon, the rate of dispersal, or straying, may be density dependent due to collective decision-making. We explore an eco-evolutionary model of two populations connected by dispersal, where the productivity of each is defined by a trait complex subject to local selection. We show that intermediate straying rates result in large gains in robustness, and that density-dependent straying promotes robustness. These results have important ramifications for the conservation of salmon metapopulations facing both natural and anthropogenic disturbances.

1. INTRODUCTION

Intraspecific diversity can increase the resilience and stability of species or metapopulations. This diversity-stability linkage can occur when there are asynchronous population dynamics, where the changes in population size varies temporally across the metapopulation. This asynchrony will increase the potential for demographic rescue [1, 2] and also decrease the variability of processes that integrate across the metapopulation [3]. For example, different responses to climate variability within populations of a rare plant reduced fluctuations in abundance [4]. This statistical buffer has traditionally been quantified as the Portfolio Effect (PE), which is the ratio of the population CV to the CV of the aggregated metapopulation [5]. Strengthened portfolio effects are expected to increase the robustness of metapopulations to external disturbances, and by extension promote persistence [5]. In contrast, homogenization of populations leading to greater synchronization and weakened PE may be a harbinger of metapopulation collapse and extinction.

Movement of individuals among local populations (i.e. dispersal) can have a large influence on metapopulation persistence [6]. Dispersal facilitates evolutionary rescue, whereby immigration of individuals with heritable adapative traits can rescue small populations from local extinction in the context of maladaptive environmental change [7, 8]. On the other hand, high rates of dispersal may synchronize populations and actually increase the risk of extinction of the entire metapopulation [2]. Third, dispersal will influence the evolutionary dynamics of the metapopulation. Although the dispersal of individuals into sites hosting other populations provides connections within the larger metapopulation, potentially promoting demographic and evolutionary rescue, it may also introduce maladapted individuals into habitats that are host to different environmental conditions, possibly lowering the mean fitness of the recipient population [9]. More broadly, dispersal can provide a mechanism by which phenotypes are sorted in space rather than time and facilitates the spread of maladaptive genes [10]. Dispersal in this case may lead to genetic homogenization that erodes the asynchrony that underpins portfolio effects and metapopulation persistence.

There is growing appreciation that a combination of abiotic, biotic, and anthropogenic factors can control the rate of dispersal among populations [11–13]. Migratory populations that return to breeding sites for reproduction are linked to each other by some proportion of the population that permanently disperses into the 'wrong' site. Recently, the role of social interactions and collective navigation has been hypothesized [14, 15, This issue]. The rate at which individuals stray, m, is in this case synonymous with dispersal and may be linked to errors made at an individual-level that are themselves diminished by migrating in groups and pooling individual choices [14–16]. The potential influence of collective dispersal on the dynamics of individual populations and the metapopulation as a whole is a topic of considerable interest that has tangible conservation implications [17–19].

The eco-evolutionary impacts of dispersal likely has important implications for conservation and management in key taxa such as in migratory salmon. While anadromous salmonid fishes (genera *Oncorhynchus* and *Salmo*) are renown for returning to their natal spawning habitats with high accuracy and precision after years at sea [12, 20, 21], there are generally some individuals that 'stray' to non-natal sites to spawn [22, 23]. Salmon may operate as metapopulations, where populations are genetically distinct but linked by some level of straying [24, 25]. Although extensive work has been done to document the extent of straying from donor populations and into recipient populations [12, 13], only recently have the abiotic, biotic, and anthropogenic influences of 'straying' behaviors been investigated systemically [26–28]. Straying among salmon may be influenced by environmental factors such as water temperature, human

activities such as hatchery practices, and population density as predicted by the collective migration hypothesis [29]. These strays can introduce new maladaptive genotypes into the recipient population. Further, straying and genetic homogenization could synchronize population dynamics and erode portfolio effects [30–32]. Thus, there is opportunity and a need to consider the eco-evolutionary consequences of straying for metapopulations in species of conservation and management concern such as salmon.

Here we seek to explore how collective density-dependent straying influences the stability and robustness of metapopulations through ecological and evolutionary processes. To address this question we construct a minimal eco-evolutionary model of two populations occupying different sites that are linked by straying individuals, each of which with an associated trait distribution subject to natural selection determined by local conditions. Specifically we compare (a) different rates of straying and (b) the influence of collective movement, across (c) increasing environmental heterogeneity, by assessing two measures of metapopulation robustness: the portfolio effect and the time required for a population(s) to recover following an induced disturbance. This model enables us to explore the multiple and potentially opposing pathways by which straying influences metapopulation robustness such as the potentially detrimental erosion of local adaptation vs. the positive effects of demographic and evolutionary rescue.

2. MODEL DESCRIPTION & ANALYSIS

(a) Metapopulation framework

We consider two populations N_1 and N_2 that inhabit two distinct habitats, each with trait values x_1 and x_2 determining recruitment rates. We assume that there is an optimum trait value θ_1 and θ_2 associated with each habitat, where recruitment is maximized if the trait value of the local population equals the optimum, such that $x = \theta$. Moreover, we assume that $x_{1,2}$ are normally distributed with means μ_1 and μ_2 and have the same standard deviation σ. As such, the recruitment rate for both populations is determined by the mean trait value of the local population, such that $r_1 = R_1[\mu_1(t), \theta_1]$. Trait means for each population are subject to selection, the strength of which depends on the difference between the trait mean and the local trait optimum at a given point in time [33, 34].

The two populations occur in spatially separate sites that are close enough such that a proportion of the population m can stray into the other site, and where mortality occurs before individuals return to reproduce. If there is no straying between these populations, then the mean trait evolves towards the optimal value for each site $x_1 \to \theta_1$, and the recruitment rate for each population is maximized. If there is straying between populations at rate m, then the traits in each respective location will be pulled away from the optimum, and recruitment rates will be lowered. As $m \to 0.5$, the populations are perfectly mixed, acting as a single population.

We use discrete Ricker framework described by Shelton and Mangel [35] as the basis for our two-site metapopulation model, with the added effect of the local population N_i mixing with a set proportion m of a remote population N_j that is straying into it. In this sense, both populations serve simultaneously as donor and recipient populations. We first assume that the proportion e^{-Z} of both populations survive such that the surviving aggregated population, composed of both local individuals (at site i) and incoming strays (from site j), is $((1-m)N_i(t) + mN_j(t))\,\mathrm{e}^{-Z}$. Because local individuals will recruit differently than incoming strays, the recruitment of the aggregate must incorporate two recruitment functions, given by $(R_i[\mu_i(t)](1-m)N_i(t) + R_i[\mu_j(t)]mN_j(t))$. This mix of individuals is subject to the same compensatory effects, which is determined by the parameter β. Taken together, the difference equation that

determine changes in population size is

$$
\begin{aligned}
&N_i(t+1) = \\
&((1-m)N_i(t) + mN_j(t))\,\mathrm{e}^{-Z} \\
&+ (R_i[\mu_i(t)](1-m)N_i(t) + R_i[\mu_j(t)]mN_j(t)) \\
&\times \mathrm{e}^{-\beta((1-m)N_i(t)+mN_j(t))},
\end{aligned}
\tag{1}
$$

where the difference equation for N_j mirrors that for N_i.

The recruitment of local individuals $(1-m)N_i(t)$ as a function of their mean trait value at time t and the local trait optimum, is

$$
\begin{aligned}
&R_i[\mu_i(t)] = \\
&\int_{-\infty}^{\infty} r_{\max} \exp\left\{\frac{(x_i(t)-\theta_i)^2}{2\tau^2}\right\} \mathrm{pr}(x_i(t), \mu_i, \sigma^2)\mathrm{d}x_i(t) + \tilde{P} \\
&= \frac{r_{\max}\tau}{\sqrt{\sigma^2+\tau^2}} \exp\left\{-\frac{(\theta_i - \mu_i(t))^2}{2\left(\sigma^2+\tau^2\right)}\right\} + \tilde{P},
\end{aligned}
\tag{2}
$$

where the mismatch between the local trait mean $\mu_i(t)$ and the local optimum θ_i scales the recruitment rate for the population, and $\tilde{P} \sim \mathrm{Normal}(0, 0.01)$ introduces a small amount of demographic error. The parameter τ is the strength of selection, and controls the sensitivity of recruitment to changes in the mean trait value away from the optimum (the strength of selection increases with smaller values of τ), which we set as $\tau = 1$ here and throughout. Because straying individuals are emigrating from a population with a mean trait value farther from the local optimum, their rate of recruitment is diminished. Recent studies of wild sockeye salmon have indeed found that straying individuals have lower life-time fitness than individuals that do not stray, although it unknown at what life-stage this selection occurs [29].

Because individuals from the local population are mixed with individuals from the remote population via straying and subsequent reproduction, the resulting trait distribution is a mixed normal with weights corresponding to the proportion of the mixed population that are local individuals, w_i, and straying individuals, $1 - w_i$, where

$$
w_i = \frac{(1-m)N_i(t)}{(1-m)N_i(t) + mN_j(t)}. \tag{3}
$$

We make two simplifying assumptions. First, we assume that the distribution resulting from the mix of remote and local individuals, following reproduction, is also normal with a mean value equal to that of the mean for the mixed-normal distribution. Thus, we assume that strays can successfully reproduce and introduce their genotypes into the recipient population, which is supported by observations in wild populations [36]. Second, we assume that changes in trait variance through time are minimal, such that σ^2 is assumed to be constant, which is a common simplification in eco-evolutionary models of population dynamics [34, 37–39].

Following Lande [34], the mean trait value thus changes through time according to the difference equation

$$\mu_i(t+1) = w_i\mu_i(t) + (1-w_i)\mu_j(t) + h^2\sigma^2\frac{\partial}{\partial\mu_i}\ln\left(w_iR_i[\mu_i(t)] + (1-w_i)R_i[\mu_j(t)]\right), \quad (4)$$

where the first two components determine the mixed normal average of the aggregated local and remote populations. The partial derivative in the Eq. 4 determines how the mean trait changes through time due to natural selection [34], which is proportional to the change in mean fitness with respect to μ_i. This model formulation has parallels to that proposed by Ronce and Kirkpatrick [40], where habitat specialization evolves between two populations as a function of dispersal. The largest difference between these approaches is that our framework treats trait evolution mechanistically at some cost to analytical tractability. Importantly, we show that the resulting dynamics are qualitatively similar, suggesting that the dynamical features present in both of these approaches have potentially widespread ramifications for the evolutionary dynamics of spatially connected populations.

(b) Density-dependent straying We have so far assumed that the proportion of strays leaving and entering a population is constant, however there is mounting evidence that at least in some species (including salmon) the straying rate is density-dependent with a signature of collective navigation [13, 15]. Specifically, the rate at which individuals stray has been linked directly to a collective decision-making phenomenon, where greater numbers of individuals tend to decrease the rate at which individuals err, reducing the overall proportion of a population that strays. According to Berdahl et al. [15, 41], given the probability that an individual strays is m_0, the proportion of the local population $N_i(t)$ that strays is

$$m(t) = m_0\left(1 - \frac{N_i(t)}{C + N_i(t)}\right), \quad (5)$$

where C is a half-saturation constant and is set to $C = 1000$ throughout. We note that at the limit $C \to \infty$, the density-dependent straying rate becomes constant such that $m(t) \to m_0$, and this corresponds to the original formulation where $m = m_0$. A similar observation shows that when the population density is very high, $m(t) \to 0$, and when it is small, individuals operate without regard to collective behavior, meaning $m(t) \to m_0$. Thus, for realistic population densities, $m(t) < m_0$.

(c) Habitat heterogeneity Increasing differences in optimal trait values between sites ($\Delta\theta = |\theta_i - \theta_j|$) corresponds to greater regional differences in the conditions that favor alternative trait complexes, which we interpret here as increased habitat heterogeneity. If both populations are isolated, natural selection will direct the mean trait values of both populations towards their respective optima, such that $\mu_i(t) \to \theta_i$ as $t \to \infty$. Although we largely treat habitat heterogeneity and the rate of straying as independent parameters, we evaluate a case where we assume that increased habitat heterogeneity correlates with lower straying rates, and vice versa (illustrated in figure S2). Two scenarios may lead to this correlation: (*i*) sites may be distributed over greater spatial distances, where habitat differences are assumed to be exaggerated and the likelihood of straying over greater distances would be lower [42, 43]; (*ii*) individuals may have behaviors promoting dispersal between habitats with structural or physiognomic similarities [29]. In this

case, the rate of straying would be greater between habitats with smaller differences in trait optima (lower $\Delta\theta$) and lesser between habitats with greater differences in trait optima (higher $\Delta\theta$).

(d) Measuring metapopulation robustness We evaluated metapopulation robustness by measuring the average-CV portfolio effect (PE) [25, 44] as well as the time required for the system to return to a steady state following an induced disturbance to one or both of the populations [45]. The average-CV portfolio effect is, as the name implies, the average CV across each population divided by the CV of the aggregate [46], such that

$$\langle \mathrm{PE} \rangle = \frac{1}{X} \sum_{i=1}^{X} \frac{\sqrt{\mathrm{VAR}(N_i^*)}}{\mathrm{E}(N_i^*)} \cdot \frac{\mathrm{E}(N_T^*)}{\sqrt{\mathrm{VAR}(N_T^*)}}, \tag{6}$$

where in this case the number of populations is limited to $X = 2$ and the expectations $\mathrm{E}(\cdot)$ and variances $\mathrm{VAR}(\cdot)$ are evaluated at the steady state. The steady state condition is denoted by '$*$'. As the CV of N_T^* decreases relative to that of the constituent populations, $\langle \mathrm{PE} \rangle > 1$, and the metapopulation is presumed to become more stable. Portfolio effects greater than unity corresponds to less synchronization [25, 47, 48] and thus a greater potential for demographic rescue among populations, buffering the system as a whole against extinction.

A more direct way to measure system robustness is to measure the time that the system (measured as the aggregate steady state biomass N_T^*) takes to recover its steady state abundance following an induced disturbance: systems that recover quickly (shorter recovery times) are more robust than those that recover more slowly (longer recovery times). Although there is a direct eigenvalue relationship between the rate of return following a small pulse perturbation [49], because we aimed to 1) assess the effects of a large perturbation, and 2) estimate the time required for all transient effects to decay (including dampened oscillations), we used a simulation-based numerical procedure. Recovery time was calculated by initiating a disturbance at $t = t_d$, and monitoring $N_T(t_d + t)$ as $t \to T$, where T is large. The aggregate was deemed recovered at t_r, such that recovery time was calculated as $t_r - t_d$, and recovery at $t = t_r$ was measured as the initial t where $N_T(t) < \mathrm{SD}\,(N_T^*)$ for $t \in (t_r, T)$, where $\mathrm{SD}(\cdot)$ is standard deviation (illustrated in figure S1).

Numerically estimating the time that it takes for a perturbed system to recover also permits a more detailed perspective of metapopulation fragility. For example, if populations settle to alternative stable states, comparing recovery times after a disturbance applied to individual populations allows for an assessment of which component of the metapopulation has a longer-lasting influence on the system's recovery. We measured recovery time following three types of induced disturbance: (*i*) extinction of the low-density population; (*ii*) extinction of the high-density population (scenarios *i* and *ii* are equivalent if populations have the same density); (*iii*) near-collapse of both populations where just 1.0% of each survives. Throughout, we will refer to an increase in the portfolio effects and/or reduction in recovery times as promoting metapopulation robustness, which promotes persistence.

3. RESULTS

(a) Nonlinear effects of straying on metapopulation robustness

Regardless of density dependence, straying lowers steady state densities for both populations by (*i*) the donor population losing locally-adapted individuals to the recipient population and (*ii*) the introduction of maladapted individuals

to the recipient population from the donor population (Fig. 1). This prediction is in accordance with observations from natural populations [13]. The decline in steady state densities is not gradual: as straying increases, the system crosses a pitchfork bifurcation (PFB) [50] whereby the single steady state for the metapopulation bifurcates into two basins of attraction: one at high biomass, and one at low biomass density (figure 1a, 2a). In discrete systems, a pitchfork bifurcation is a specific case of the cusp bifurcation (which occurs when two fold bifurcations intersect at a cusp), which occurs when the real part of the dominant eigenvalue of the Jacobian matrix crosses the unit circle at $+1$, which we show in figure S3.

Mean trait values for both populations bifurcate similarly (figure 1b), depending on which population attains a low- vs. high-density. Above the threshold straying rate defined by the PFB, there are two alternative eco-evolutionary states: the *dominant state* population will have a higher density and higher degree of local adaptation (smaller trait offset from the local optimum), while the *subordinate state* population will have lower density with maladapted trait values (larger trait offset from the local optimum). Hysteresis is observed to occur at this transition, such that the single steady state regime cannot be easily recovered by lowering m after the system attains alternative steady states (figure S4). These dynamics are also observed in the Ronce and Kirkpatrick model, where populations are described as transitioning between symmetric to asymmetric states [40]. Whether a specific population goes to one state or the other in our model is random, due to a small amount of introduced variance in the initial conditions.

Trait heritability has a large impact on the degree to which straying affects both the aggregate population steady state density ($N_T^* = N_1^* + N_2^*$; figure 2a) as well as the difference between steady state densities (the distance between alternative stable states: $\Delta N^* = |N_1^* - N_2^*|$; figure 2b). Greater trait heritability results in a faster decline in N_T^* with increasing straying rates m, but leads to only moderate changes to ΔN^*. Conversely, in the context of lower trait heritability, an increase in the straying rate has little impact on the total biomass density but contrastingly large effects on ΔN^*. The pitchfork bifurcation (the black line in Figs. 2a-c) occurs at lower values of the straying rate m with decreased trait heritability h^2 (Fig 2a,b), indicating that weaker coupling between ecological and evolutionary dynamics in addition to higher rates of straying promotes the appearance of alternative stable states. Although trait heritability among salmonids is variable, most life history traits have an $h^2 < 0.5$ [51], and we largely focus additional analyses on that range.

As the pitchfork bifurcation is approached with increasing m, the portfolio effect increases sharply due to an amplification in variance within both donor and recipient populations. This amplification in variance is the product of a dynamical process known as *critical slowing down* that occurs near pitchfork bifurcations [52], a phenomenon that some have suggested may serve as an early warning indicator for approaching phase transitions [52–56]. For larger values of m (to the right of the pitchfork bifurcation in Fig 2a-c), where alternative stable states occur, the portfolio effect declines steadily as the CV of N_T^* increases. The decline over m is more gradual if trait heritability is low, and steeper if trait heritability is high (figure 2c).

As the portfolio effect is highly sensitive to the rate of straying between populations, so is the time required for the system to recover to a steady state following a large disturbance. In general, we find that the average-CV portfolio effect is negatively correlated with recovery time (figure 2d), indicating that, for our system, both measures are valuable indicators of metapopulation robustness. Because we can assess the time to recovery in response to the various disturbance types described above, this allows us to gain an in-depth perspective into the fragility of the metapopulation as a function of straying rate.

Straying had non-linear impacts on the recovery time of populations. When the dominant state (well adapted and high density) is wiped out, high levels of straying allow it to recover quickly (figure 4a) because the surviving population has a mean trait value skewed towards the optimum of the recovering population (figure S6). Yet, as straying decreases, recovery time for the disturbed dominant state population increases, in part because there is enough time for the trait distribution to move back towards the trait optimum of the subordinate state population. In contrast, when the subordinate state population (maladapted and low density) is wiped out, recovery rates are fastest at low to intermediate levels of straying. Because the mean trait values of both populations are skewed towards those of the dominant population, when the subordinate population collapses under high rates of straying, selection against the flood of maladapted individuals that stray into the recovering population extends the length of time required for it to return to its steady state (figure S5). When both populations are both dramatically reduced, recovery time is generally fastest at lower levels of straying, while near the onset of the pitchfork bifurcation, recovery time increases explosively and this is – as the name implies – characteristic of *slowing* dynamics that occur near critical transitions [52, 57].

(b) The effects of collective migration and density dependent straying

If we assume that the rate of straying is density-dependent, the probability that an individual strays m_0 determines the rate of straying within the population, such that $m(t)$ becomes lower as $N(t)$ increases, likely due to the effects of collective decision-making [15] (Eq. 5). Density dependence alters the straying rate at steady state population densities because $0 < m^* < m_0$, and this serves to rescale both the strength of the PE as well as the recovery time, but does not change the qualitative nature of our findings. In the alternative stable state regime, because each population exists at different steady state densities, there are likewise two alternative straying rates (m_i^*, m_j^*): the higher straying rate is associated with the low-density population, and the lower straying rate is associated with the high-density population. We assessed metapopulation robustness across a range of (m_i^*, m_j^*) values by varying the probability that an individual strays m_0, which is positively and linearly related to (m_i^*, m_j^*). We find that the portfolio effects generated in systems with density-dependent straying are qualitatively similar to systems with constant straying, however there are some important quantitative differences. First, the PE associated with the high-density (low m^*) population is the same as that for a system with a constant m (figure 3a). As m^* increases, we observe an increase in the PE than for systems with constant m.

Density-dependent straying alters these recovery times (figure 4b). First, in comparison with constant stray rates, density-dependent straying made recovery more rapid at elevated stray rates when both populations collapsed and when the subordinate population was extirpated. At low straying rates, near-collapse of both populations resulted in longer than expected recovery times, whereas in the alternative stable state regime (higher m^*), the recovery times for different disturbance types were very similar to systems with a constant m (figure 4b; note difference in x-axis scales). As trait heritability increased, the metapopulation always recovered more quickly if the small population was lost (figure S7). The lower recovery time for systems with increased m^* mirrors an elevated PE with higher density-dependent straying rates (figure 3). In tandem, analysis of both PE and recovery time suggests that although density-dependent straying does not appear to change the 'dynamic landscape' in our minimal model, it does appear to promote robustness, particularly when the aggregate biomass is low and straying is correspondingly high.

Increased rates of straying lowers phenotypic diversity ($\Delta\mu^* = |\mu_i^* - \mu_j^*|$, evaluated at the steady state) because both local and remote populations are increasingly homogenized. The loss of phenotypic diversity with increased

straying is greater if trait heritability is low because traits take longer to go back to their local optima than they do when heritability is large. Hence straying counters the effect of diversifying local adaptation. Less intuitively, we observe a discrete jump towards low phenotypic diversity as the pitchfork bifurcation is crossed (figure 5). Although the development of alternative stable states elevates the portfolio effect due to the variance-dampening effects of the aggregate, entering this dynamic regime also results in a substantial decline in phenotypic diversity, which may have less predictable adverse effects on the population.

(c) The role of habitat heterogeneity and changing selective landscapes

With the onset of straying, we find that increasingly divergent trait optima generally lower N_T^* and exaggerate ΔN^* (figure S8), such that the biomass distribution becomes increasingly uneven. The impact of habitat heterogeneity on the portfolio effect and recovery time is more complex, serving to emphasize the nonlinear relationship between rates of straying and metapopulation robustness. As habitat heterogeneity increases, alternative stable states appear at lower straying rates – with the crossing of the pitchfork bifurcation, accompanied by a peak in the PE – whereas the magnitude of increase in the PE also increases (figure 3b), reducing recovery time (figure S9). For increased rates of straying, greater habitat heterogeneity erodes the PE (figure 3b) and increases the recovery time (figure S9). These results together suggest that habitat heterogeneity, as measured as the differences in trait optima between two habitats $\Delta\theta$, promotes robustness when straying rates are low, and erodes robustness when straying rates are high.

Sites that are farther apart are likely to be more heterogeneous, while simultaneously facilitating lower rates of straying between populations. We implemented this dependence as set $m, m_0 = 0.5(1 + \Delta\theta)^{-1}$ where maximum straying is assumed to occur at $m = 0.5$ (perfect mixing; figure S2). This assumes that m or m_0 increases in situations where $\Delta\theta$ is lower, such that there are low rates of straying between dissimilar sites and high straying rates between similar sites. We find that under these conditions alternative stable states now appear for very low rates of straying $0 < m \leq 0.43$. As the straying rate increases and $\Delta\theta$ decreases, a single stable state emerges as the pitchfork bifurcation is crossed, which is opposite the pattern observed when these parameters are independent.

There are two notable dynamics that emerge following extinction of the dominant population at low rates of straying between dissimilar (high $\Delta\theta$) sites: (i) above a threshold m value, the dominant population recovers quickly enough that the evolving subordinate phenotype is overwhelmed by incoming strays, and it shifts back to its pre-disturbance (subordinate) state; (ii) below a threshold m value, there is an *inversion* between subordinate and dominant states: because there is enough time and isolation for the subordinate trait mean to shift towards its local optimum, and away from that of the recovering dominant population, the dominant population becomes subordinate, and the subordinate population becomes dominant (figure S11). This threshold value of m, below which the inversion dynamic behavior occurs, is marked by the asterisk in figure 6, and holds for both constant and density-dependent straying (figure S12).

4. DISCUSSION

We have shown that density-dependent straying between populations consistent with collective navigation, coupled with localized selection against donor phenotypes, has a large and nonlinear impact on dynamic properties that affect metapopulation robustness. We measured robustness as: 1) the average-CV portfolio effect [3, 46], a statistical metric commonly used to assess the buffering capacity of metapopulations, and 2) the recovery time, defined here as the time

required for the aggregate metapopulation biomass N_T^* to return to its steady state following an induced disturbance, which is mechanistically linked to persistence [45]. In our minimal eco-evolutionary model of dispersal and natural selection between two populations, we show that these statistical and mechanistic descriptors of metapopulation dynamics and robustness are tightly coupled (figure 2d), which is not uncommon for diverse metrics of stability [58]. Taken as a whole, our results point to an important role of density-dependent straying in the colonization and recovery dynamics within metapopulations, while also underscoring the risk of straying by individuals with maladaptive traits to reduce the productivity of locally adapted stock complexes.

A salient finding from our results is that straying can lead to the emergence of alternative stable states, pushing one of the populations to high density (the *dominant state*), and one to low density (the *subordinate state*). This pattern has been observed in other models of eco-evolutionary dynamics with explicit space [40], suggesting that it may be a general feature of spatially-linked traits that evolve toward local optima while being hindered by dispersal. An important quality of our framework is that there are similar forces that dictate interactions within and between sites, and this naturally results in a symmetry that could preclude the relevance of our finding for natural (and inherently less symmetric) systems. Although the emergence of alternative stable states via a pitchfork bifurcation is characteristic of symmetrical systems, we find that increasing the asymmetry in the vital rates of populations across sites does not alter the presence or position of the PFB (figure S13). That these patterns arise in alternative formulations and are insensitive to parameter asymmetry suggests that the emergence of dominant and subordinate states directly from eco-evolutionary dynamics may be a generally relevant phenomenon in ecological systems.

An intermediate straying rate maximizes metapopulation robustness. Results from our model reveal that the presence of just enough straying to cause formation of alternative stable states increases the portfolio effect (figure 2a). Previous theoretical work has shown that increased connectivity may erode portfolio effects in herring metapopulations, where straying is also thought to be density-dependent [63]. Although high levels of dispersal in our system generally supports this finding, the interplay between dispersal and PE is more subtle when selection for local adaptations is considered, such that low to intermediate levels of density-dependent straying result in an elevated PE, thus increasing the buffering capacity of the metapopulation. Although PE is measured at the steady state, low to intermediate rates of straying also appear to have a beneficial effect on transient dynamics. When there is just enough straying to cause alternative stable states, the time to recovery following an induced disturbance declines, though – as with the PE – recovery time then grows if straying becomes very large (figure 4a).

This themed issue formalizes the role of collective movement in the ecology of natural systems and illuminates a signature of collective navigation in animal populations on the move. We observed three salient results that contribute to our understanding of collective movement that combine to suggest that density-dependent straying may play an important role in the persistence of metapopulations over evolutionary time. First, the inclusion of density-dependent straying does not qualitatively alter either (*i*) steady state or (*ii*) transient dynamics of our minimal eco-evolutionary model, but effectively rescales measures of robustness to the lower straying rates that emerge as a consequence of the coupled dynamics. Second, compared to systems with constant dispersal, density-dependent straying appears to increase the portfolio effect across a range of straying rates (figure 3a). Third, density-dependent straying reduces the time to recovery following disturbance, and this is particularly true in the case of near-collapse of the metapopulation (figure 4b). In the case of near-collapse, although both populations inherit low population densities, the mean trait values of both are skewed towards the optimum of the dominant population. Due to density-dependent straying, low

population densities lead to greater dispersal, and while this increased connectivity primarily facilities the growth of the dominant population (because the trait means are closer to the dominant optimum), because the dominant population contains the bulk of the aggregate biomass, the overall recovery time is lessened significantly (figures 4b, S14).

Salmon are distributed and stray across a diverse range of habitats, and the rates of straying between geographically diverse sites can be plastic and idiosyncratic [27]. Our surrogate measure for habitat heterogeneity is the difference in trait optima between sites $\Delta\theta$. In general, our findings indicate that increased habitat heterogeneity promotes robustness (higher PE, shorter time to recovery) when straying rates are low, but may erode robustness when straying rates are high (figure 3b, solid lines). This may be particularly consequential for populations that are spatially adjacent but separated by sharp environmental boundaries, such that trait optima are divergent yet dispersal is relatively high. Such a scenario plays out repeatedly in the context of adjacent wild and hatchery-produced salmon. Although wild and hatchery populations may occur close on the landscape, and indeed often are sympatric within the same river network, the selective environments to which they are locally adapted differ dramatically [64]. Straying of domesticated hatchery-produced fish from release sites and spawning in the wild drastically reduces the productivity of wild populations through competition and outbreeding depression [65, 66].

All else being equal, habitats that are closer in space generally have greater similarity in environmental conditions than habitats that are geographically distant, and correspondingly phenotypes of more proximately located populations should be more similar to those that are distant [67]. It is thus reasonable to expect a larger number of straying individuals between sites that are geographically proximate and indeed evidence corroborates this prediction [42, 43]. Alternatively, salmon that cue to specific environmental conditions may be more likely to stray into sites that have structurally and physiognamically similar habitats [29] even if other potential sites are closer. These considerations justify imposing a direct relationship between the rate of straying m and habitat heterogeneity: as site dissimilarity increases, so too should the straying rate decrease. When habitat heterogeneity and the rate of straying are linked in this way, we show that very small amounts of either constant or density-dependent straying result in long recovery times for the dominant population because there is time for selection to push the subordinate trait mean away from the optimum of the dominant population (figure 6). If the straying rate is very low, there is an inversion in the alternative stable states following the disturbance, resulting in a state shift in dominance. This may have particular conservation implications for considerations of aiding dispersal following disturbances or reconnections of lost habitats [68, 69].

Although our study was inspired by salmon metapopulations, the results have general implications for the conservation and management of other migratory metapopulations as well. Because changes in straying rates can have large and nonlinear impacts on robustness, human activities that alter straying rates could have unintended consequences. For example, salmon produced by hatcheries often stray into proximate wild populations [17], and these recipient populations can have lower fitness due in part to the introduction of maladapted genes [70]. We show that there is an intermediate straying rate where disturbed populations that are recovering by the introduction of maladapted strays recover fastest: if the straying rate is too low or too high, recovery times increase (figure 4). This finding suggests that salmon stocking efforts that aim to lower recovery times following dam removal could actually prolong recovery if the rate at which individuals are introduced is not taken into account. Ongoing examinations of experimental restocking in the recently re-opened Elwha River (Washington State) will provide empirical insight into the potential short- and

long-term consequences of facilitated recovery [71].

The portfolio effect and the time to recovery following a disturbance are independent and correlated measures of metapopulation robustness that take into account both steady state and transient dynamics. We show that these measures of robustness are strongly influenced by the rate at which individuals from donor populations stray into habitats occupied by recipient populations. Importantly, density-dependent straying, which may occur when individuals collectively navigate, can both increase the portfolio effect and lower the time to recovery following a disturbance, which is anticipated to promote persistence. We suggest that understanding the spatial complexity of metapopulations dispersing across heterogeneous environments, in tandem with the mosaic of selective forces acting on those environments, may be key to uncovering those factors that promote persistence in the wild.

Competing interests: The authors declare no competing interests

Author contributions: JDY and JWM conceived of the initial project design. JDY and JPG designed the modeling framework and conducted the analyses. JDY, JPG, PAHW, and JWM interpreted the results, and drafted and wrote the manuscript.

Data Accessibility: Code is made available at https://github.com/jdyeakel/SalmonStrays

Acknowledgements: We thank Sean Anderson for helpful discussions and comments on the manuscript. We also thank the guest editors Andrew Berdahl, Dora Biro, and Colin Torney, for inviting us to contribute to this themed issue. J.D.Y. was supported by startup funds at the University of California, Merced, and an Omidyar Postdoctoral Fellowship at the Santa Fe Institute. J.P.G. was supported by a James S. McDonnell Foundation Postdoctoral Fellowship in Complex Systems at the University of California, Merced. P.A.H.W. was supported by the UA Foundation at the University of Alaska Fairbanks. J.W.M. was supported by the Liber Ero Research Chair in Coastal Science and Management at Simon Fraser University.

[1] J. H. Brown and A. Kodric-Brown, Ecology **58**, 445 (1977).

[2] D. J. D. Earn, S. A. Levin, and P. Rohani, Science **290**, 1360 (2000).

[3] D. E. Schindler, J. B. Armstrong, and T. E. Reed, Front. Ecol. Environ. **13**, 257 (2015).

[4] R. E. Abbott, D. F. Doak, and M. L. Peterson, Ecology **98**, 1071 (2017).

[5] L. M. Thibaut and S. R. Connolly, Ecol. Lett. **16**, 140 (2013).

[6] E. J. Milner-Gulland, J. M. Fryxell, and A. R. E. Sinclair, *Animal Migration* (Oxford University Press, Oxford, 2011).

[7] G. Bell and A. Gonzalez, Science **332**, 1327 (2011).

[8] S. M. Carlson, C. J. Cunningham, and P. A. H. Westley, Trends Ecol. Evol. **29**, 521 (2014).

[9] C. C. Muhlfeld, R. P. Kovach, L. A. Jones, R. Al-Chokhachy, M. C. Boyer, R. F. Leary, W. H. Lowe, G. Luikart, and F. W. Allendorf, Nature Climate Change **4**, 620 (2014).

[10] W. H. Lowe, C. C. Muhlfeld, and F. W. Allendorf, Trends Ecol. Evol. **30**, 456 (2015).

[11] P. A. H. Westley and T. P. Quinn, Can. J. Fish. Aquat. Sci. **70**, 735 (2013).

[12] M. L. Keefer and C. C. Caudill, Rev Fish Biol Fisher **24**, 333 (2014).

[13] N. N. Bett, S. G. Hinch, N. J. Burnett, M. R. Donaldson, and S. M. Naman, Fisheries **42**, 220 (2017).

[14] A. Berdahl, C. J. Torney, E. Schertzer, and S. A. Levin, Evolution **69**, 1390 (2015).

[15] A. Berdahl, Movement Ecology **4**, 1 (2016).

[16] A. M. Simons, Trends Ecol. Evol. **19**, 453 (2004).

[17] R. E. Brenner, S. D. Moffitt, and W. S. Grant, Environ Biol Fish **94**, 179 (2012).

[18] R. C. Johnson, P. K. Weber, J. D. Wikert, M. L. Workman, R. B. MacFarlane, M. J. Grove, and A. K. Schmitt, PLoS ONE **7**, e28880 (2012).

[19] A. H. Fullerton, S. T. Lindley, G. R. Pess, B. E. Feist, E. A. Steel, and P. Mcelhany, Conserv Biol **25**, 932 (2011).

[20] T. P. Quinn, *The Behavior and Ecology of Pacific Salmon and Trout* (UBC Press, Vancouver, 2011).

[21] B. Jonsson and N. Jonsson, *Ecology of Atlantic Salmon and Brown Trout* (Springer Netherlands, Dordrecht, 2011).

[22] T. P. Quinn, Fish Res **18**, 29 (1993).

[23] A. P. Hendry, T. Bohlin, B. Jonsson, and O. K. Berg, in *Evolution Illuminated*, edited by A. P. Hendry and S. C. Stearns (Oxford University Press on Demand, Oxford, 2004).

[24] N. Schtickzelle and T. P. Quinn, Fish Fish. **8**, 297 (2007).

[25] S. C. Anderson, J. W. Moore, M. M. McClure, N. K. Dulvy, and A. B. Cooper, Ecol. Appl. **25**, 559 (2015).

[26] M. L. Keefer, C. C. Caudill, C. A. Peery, and S. R. Lee, Ecol. Appl. **18**, 1888 (2008).

[27] P. A. H. Westley, A. H. Dittman, E. J. Ward, and T. P. Quinn, Ecology **96**, 2823 (2015).

[28] M. H. Bond, P. A. H. Westley, A. H. Dittman, D. Holecek, T. Marsh, and T. P. Quinn, T Am Fish Soc **146**, 60 (2016).

[29] D. A. Peterson, R. Hilborn, and L. Hauser, Nat Commun **5**, 3696 (2014).

[30] J. W. Moore, M. McClure, L. A. Rogers, and D. E. Schindler, Conserv. Lett. **3**, 340 (2010).

[31] S. M. Carlson, W. H. Satterthwaite, and I. A. Fleming, Can. J. Fish. Aquat. Sci. **68**, 1579 (2011).

[32] D. C. Braun, J. W. Moore, J. Candy, and R. E. Bailey, Ecography **39**, 317 (2016).

[33] G. G. Simpson, *The Major Features of Evolution* (Simon and Schuster, New York, 1953).

[34] R. Lande, Evolution **30**, 314 (1976).

[35] A. O. Shelton and M. Mangel, Proc. Natl. Acad. Sci. USA **108**, 7075 (2011).

[36] J. R. Jasper, C. Habicht, S. Moffitt, R. Brenner, J. Marsh, B. Lewis, E. C. Fox, Z. Grauvogel, S. D. R. Olive, and W. S. Grant, PLoS ONE **8**, e81916 (2013).

[37] S. J. Schreiber, R. Bürger, and D. I. Bolnick, Ecology **92**, 1582 (2011).

[38] J. P. Gibert and C. E. Brassil, Ecol Evol **4**, 3703 (2014).

[39] J. P. Gibert and J. P. DeLong, Adv Ecol Res **52**, 45 (2015).

[40] O. Ronce and M. Kirkpatrick, Evolution **55**, 1520 (2001).

[41] A. Berdahl, P. A. H. Westley, S. A. Levin, I. D. Couzin, and T. P. Quinn, Fish Fish. **17**, 525 (2014).

[42] J. R. Candy and T. D. Beacham, Fish Res **47**, 41 (2000).

[43] R. S. Schick and S. T. Lindley, J. Appl. Ecol. **44**, 1116 (2007).

[44] D. E. Schindler, J. B. Armstrong, and T. E. Reed, Front. Ecol. Environ. **13**, 257 (2015).

[45] O. Ovaskainen and I. Hanski, Theor Popul Biol **61**, 285 (2002).

[46] S. C. Anderson, A. B. Cooper, and N. K. Dulvy, Methods Ecol Evol **4**, 971 (2013).

[47] M. Loreau and C. de Mazancourt, Am. Nat. **172**, E48 (2008).

[48] J. D. Yeakel, J. W. Moore, P. R. Guimarães Jr, and M. A. M. de Aguiar, Ecol. Lett. **17**, 273 (2014).

[49] J. Guckenheimer and P. Holmes, *Nonlinear Oscillations, Dynamical Systems, and Bifurcations of Vector Fields* (Springer, New York, 1983).

[50] Y. Kuznetsov, *Elements of applied bifurcation theory* (Springer, New York, 1998).

[51] S. M. Carlson and T. R. Seamons, Evol Appl **1**, 222 (2008).

[52] M. Scheffer, J. Bascompte, W. A. Brock, V. Brovkin, S. R. Carpenter, V. Dakos, H. Held, E. H. van Nes, M. Rietkerk, and G. Sugihara, Nature **461**, 53 (2009).

[53] S. J. Lade and T. Gross, PLoS Comp. Biol. **8**, e1002360 (2012).

[54] C. Boettiger, N. Ross, and A. Hastings, Theor. Ecol. **6**, 255 (2013).

[55] V. Dakos and J. Bascompte, Proc. Natl. Acad. Sci. USA **111**, 17546 (2014).

[56] M. Krkošek and J. M. Drake, Proc. Roy. Soc. B **281**, 20133221 (2014).

[57] C. Kuehn, Physica D **240**, 1020 (2011).

[58] I. Donohue, O. L. Petchey, J. M. Montoya, A. L. Jackson, L. McNally, M. Viana, K. Healy, M. Lurgi, N. E. O'Connor, and M. C. Emmerson, Ecol. Lett. **16**, 421 (2013).

[59] S. A. Levin, Ecology **73**, 1943 (1992).

[60] H. Meinhardt, Interface Focus **2**, 407 (2012).

[61] I. Hanski, *Metapopulation Ecology* (Oxford University Press, Oxford, 1999).

[62] D. A. Boughton, Ecology **80**, 2727 (1999).

[63] D. H. Secor, L. A. Kerr, and S. X. Cadrin, ICES J Mar Sci **66**, 1726 (2009).

[64] M. R. Christie, M. L. Marine, R. A. French, and M. S. Blouin, Proc. Natl. Acad. Sci. USA **109**, 238 (2012).

[65] M. W. Chilcote, Can. J. Fish. Aquat. Sci. **60**, 1057 (2003).

[66] H. Araki, B. Cooper, and M. S. Blouin, Science **318**, 100 (2007).

[67] P. A. H. Westley, Corinne M. Conway, and I. A. Fleming, Evol. Ecol. Res. **14**, 147 (2012).

[68] J. H. Anderson, P. L. Faulds, W. I. Atlas, and T. P. Quinn, Evol Appl **6**, 165 (2013).

[69] G. R. Pess, T. P. Quinn, S. R. Gephard, and R. Saunders, Rev Fish Biol Fisher **24**, 881 (2014).

[70] M. J. Ford, Conserv Biol **16**, 815 (2002).

[71] M. Liermann, G. PESS, M. McHenry, J. McMillan, M. Elofson, T. Bennett, and R. Moses, T Am Fish Soc **17**, 1 (2017).

Parameter	Definition
$N_i(t)$, $N_T(t)$	Individual, aggregate population over time
$\mu_i(t)$	Mean trait value of population i over time
m, $m(t)$	Constant, density dependent straying rate
m_0	Straying rate of an individual
$R_i[\mu(t)]$	Recruitment rate of population i
$r_{\max}$	Maximum recruitment rate
e^{-Z}	Survival rate
β	Strength of density dependence
θ_i	Optimal trait value for habitat i
$\Delta\theta$	Habitat heterogeneity
τ	Strength of selection
σ^2	Genetic variance
h^2	Heritability
C	Half saturation constant for $m(t)$
PE	Portfolio Effect

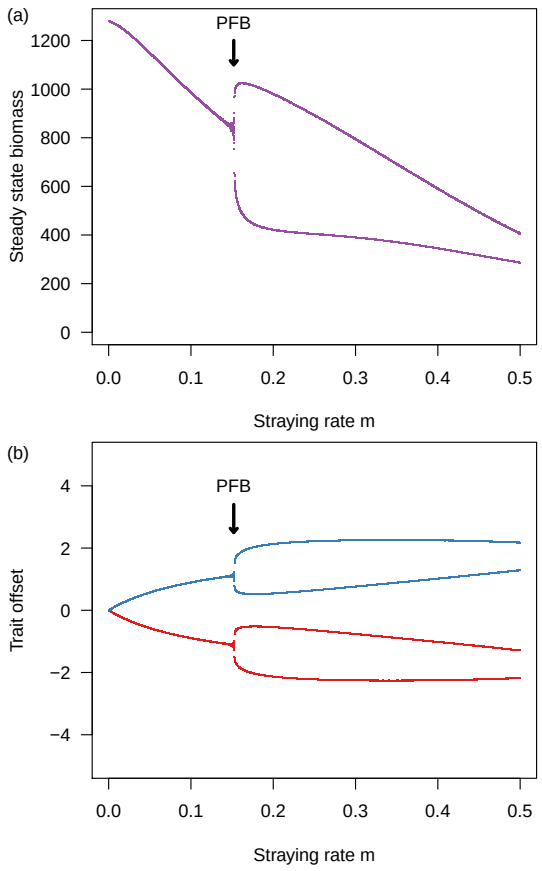

Figure 1: (a) The steady state densities of N_1 and N_2 as a function of a constant stray rate m. Which population attains the low- or high-density state is random due to small applied fluctuations in the initial conditions. (b) The steady state trait values measured as $\theta_i - x_i$, as a function of a constant stray rate m. PFB marks the pitchfork bifurcation. Unless otherwise indicated, the default parameter values used are: $r_{\max} = 2$; $Z = 0.5$; $\beta = 0.001$; $\theta_1 = 5$; $\Delta\theta = 5$; $\tau = 1$; $\sigma = 1$; $T = 1 \times 10^5$.

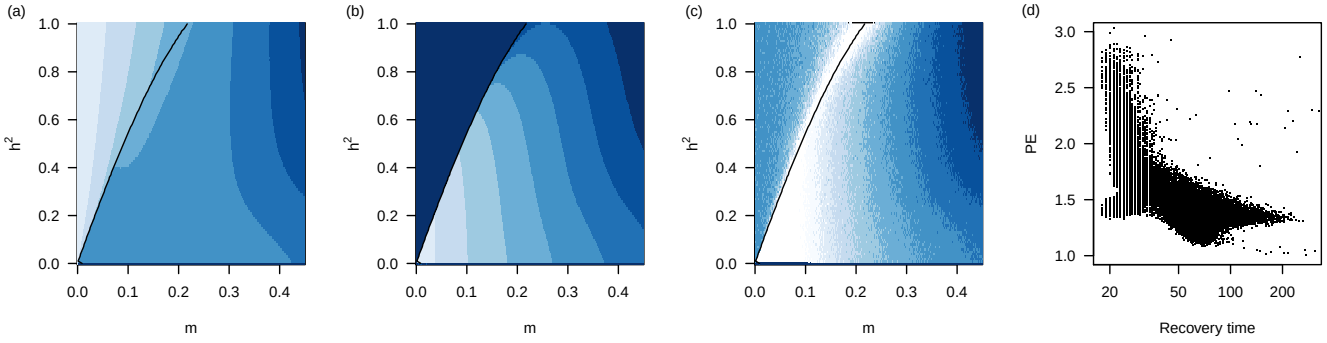

Figure 2: (a) Total means N_t^*, (b) difference in means ΔN^*, and (c) the portfolio effect PE as a function of heritability h^2 and a constant stray rate m. Light colors = high values. The black line shows the pitchfork bifurcation separating a single steady state (left) from alternative stable states (right). (d) The relationship between the time to recovery following a disturbance and the portfolio effect. Portfolio effects greater than unity corresponds to less synchronization. The black line denotes the pitchfork bifurcation.

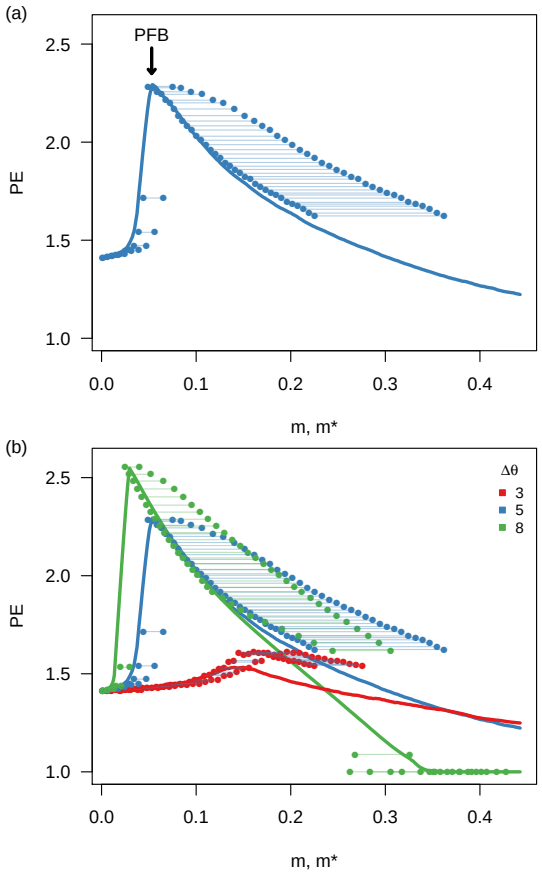

Figure 3: (a) Median portfolio effect as a function of a constant stray rate m (solid line) and density-dependent stray rate (point pairs) given heritability is $h^2 < 0.5$ and $\Delta\theta = 5$. Point pairs connected by a horizontal line represent the PE as a function of density-dependent straying rates, evaluated for both low- and high-density populations at equilibrium. The lower straying rate of a pair is for the larger population; the higher straying rate is for the smaller population. (b) Median portfolio effects for habitats with increasing heterogeneity as measured by the difference in regional trait optima $\Delta\theta$ for both constant and density-dependent stray rates as shown in (a). Portfolio effects greater than unity corresponds to less synchronization. PFB marks the pitchfork bifurcation.

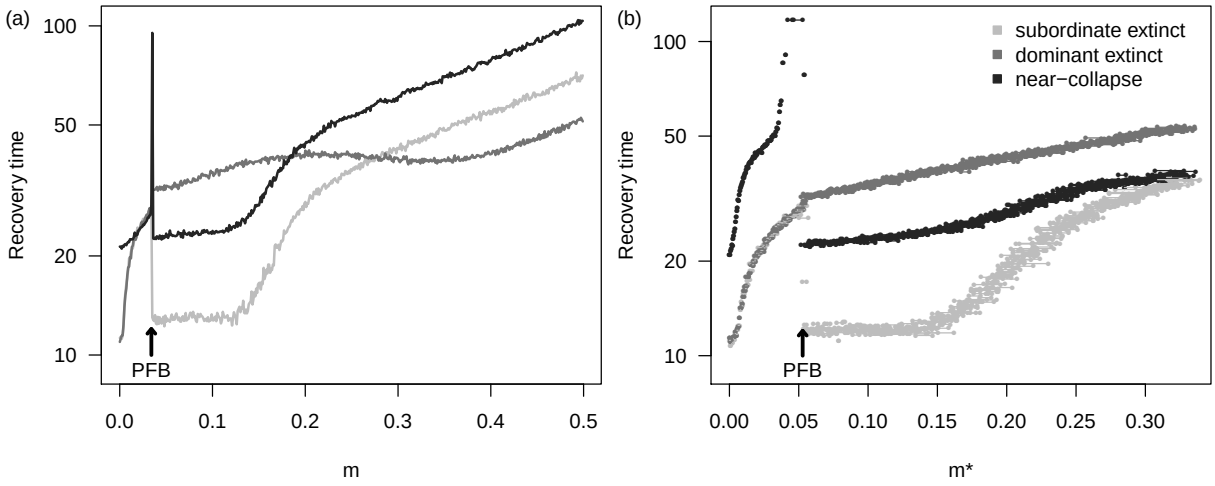

Figure 4: Recovery time of N_T^* following the extinction of either the low-density (light gray) or high-density (gray) population, or the near-collapse of both (dark gray) assuming (a) constant straying rates m and (b) density-dependent straying rates (evaluated at the steady state m^*) with trait heritability $h^2 = 0.2$. If m is density-dependent, in the alternative stable state regime there are two straying rates observed: one each for the low- and high-density populations, respectively, which are linked by a horizontal line. PFB marks the pitchfork bifurcation.

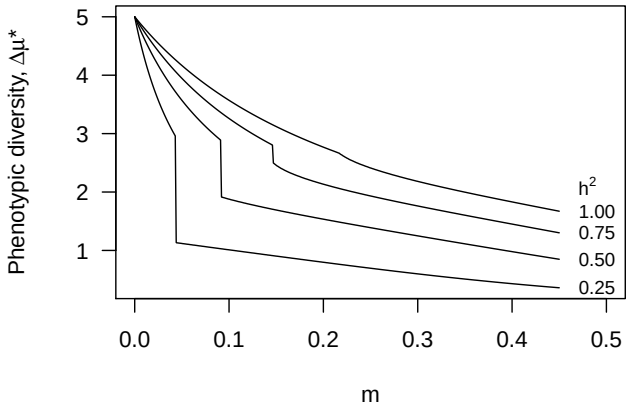

Figure 5: Phenotypic diversity ($\Delta\mu^*$) evaluated at the steady state as a function of straying rate m and trait heritability h^2. The descrete jump occurs as the system crosses the pitchfork bifurcation; lower phenoytic diversity emerges with higher straying rates and in the alternative stable state regime.

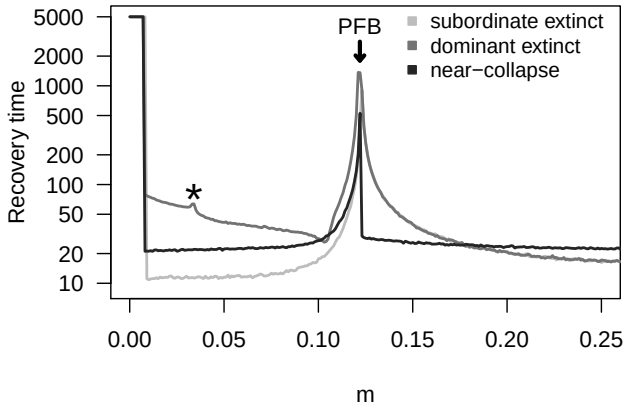

Figure 6: Distance dependent recovery times for three disturbance types. When straying is distance dependent, m increases as $\Delta\theta$ decreases. The '$*$' marks the value of $(m, \Delta\theta)$ below which there is a switch in subordinate/dominant states following extinction of the dominant population. PFB marks the pitchfork bifurcation.

Figure S1: Example of the numerical procedure used to estimate recovery time. After a disturbance is introduced, the recovery time is calculated by measuring the point in time where N_T (in black), which is the aggregate of both populations (blue, red) settles to within one standard deviation of the new equilibrium N_T^*.

Figure S2: In some cases, habitat heterogeneity may be assumed to determine the rate of straying, if for example: 1) sites may be distributed over greater spatial distances, where habitat differences are assumed to be greater between more distant sites, or 2) individuals have behaviors promoting dispersal between habitats that are more similar. To examine such cases, we use the relationship $m = 0.5(1 + \Delta\theta)^{-1}$ where maximum straying is assumed to occur at $m = 0.5$ (perfect mixing).

Figure S3: The real parts of the four eigenvalues for the Jacobian matrix of the 4-dimensional system. The pitchfork bifurcation occurs when the dominant eigenvalue crosses the unit circle at +1.

Figure S4: Increasing the straying rate results in the transition from a single steady state for both populations to a dominant and subordinate states. If the straying rate is subsequently lowered, the single steady state is not easily obtained, which is the hallmark of hysteresis.

Figure S5: Extinction of low-density population with a high constant straying rate $m = 0.4$ and low trait heritability $h^2 = 0.2$ (see figure 4a). Black line marks the calculated point of recovery post-perturbation. Trait optima are $\theta_1 = 10$ (blue population trajectory) and $\theta_2 = 5$ (red population).

Figure S6: Extinction of high-density population with a high straying rate $m = 0.4$ and low trait heritability $h^2 = 0.2$ (see figure 4a). Black line marks the calculated point of recovery post-perturbation. Trait optima are $\theta_1 = 10$ (blue population trajectory) and $\theta_2 = 5$ (red population).

Figure S7: Recovery time of N_T following the extinction of either the low-density (light gray) or high-density (gray) population, or the near-collapse of both (dark gray) assuming (a) constant straying rates m and (b) density-dependent straying rates (evaluated at the steady state m^*) with trait heritability $h^2 = 0.8$. If m is density-dependent, in the alternative stable state regime there are two straying rates observed: one each for the low- and high-density populations, respectively, which are linked by a horizontal line.

Figure S8: Median difference in population densities taken over the straying rate as a function of habitat heterogeneity $\Delta\theta$. Solid lines are for constant m; dashed lines are for density-dependent m

Figure S9: (a) Recovery time after near collapse of both populations as a function of straying rate m and habitat heterogeneity $\Delta\theta$. (b) The same as (a) but including recovery times when straying is density-dependent, shown by linked pairs of points. Recovery times for systems with density-dependent straying are longer at low straying rates and shorter at higher straying rates, mirroring the change in portfolio effects shown in figure 3.

Figure S10: Distance dependent portfolio effects as a function of straying rate m and trait heritability h^2. When straying is distance dependent, m increases as $\Delta\theta$ decreases.

Figure S11: Distance dependent straying, where increased differences in trait optima between sites $\Delta\theta$ corresponds to lower rates of straying m. At low rates of straying $m = 0.02$ ($\Delta\theta = 24$), extinction of the dominant population leads to slower-than-expected recovery times because the subordinate population is isolated enough to evolve towards its own trait optimum. In this case, m is less than $m = 0.034$ (denoted by the asterisk in figure 6), such that isolation allows the subdominant population to 'run away' from the influence of the dominant population, leading to a switch in states. If m is low but greater than 0.034, isolation permits the subdominant population to 'run away' from the influence of the dominant population, until it is overwhelmed by the recovering dominant population, and reverts back to its previous trait mean prior to the disturbance.

Figure S12: Distance dependent recovery times for three disturbance types. When straying is distance dependent, m increases as $\Delta\theta$ decreases for constant (a) and density-dependent (b) staying rates. The pitchfork bifurcation is not as clear in (b) because $\Delta\theta$ is a function of the individual straying rate m_0, whereas the x-axis in (b) is the straying rate at the steady state m^*. Despite this difference, the general trends shown in (a) are also present in (b).

Figure S13: Steady state densities of both populations as a function of m, where a pitchfork bifurcation indicates the emergence of alternative steady states: one in a dominant state and one in a subordinate state. Steady states for populations with symmetrical values ($\alpha = 0$) in the vital rates $r_{\max}$ and β are shown with cool tones. As the asymmetry among populations between sites increases ($\alpha > 0$), their vital rates diverge, such that the maximal growth at sites 1 and 2 is now $r_{\max}(1) = r_{\max}(1 + \tilde{rv}_1)$ and $r_{\max}(2) = r_{\max}(1 + \tilde{rv}_2)$ where $rv_{1,2}$ are independently drawn from Normal$(0, \alpha)$ and $r_{\max} = 2$. Similarly the strength of density dependence is calculated at sites 1 and 2 as $\beta(1) = \beta(1 + \tilde{rv}_1)$ and $\beta(2) = \beta(1 + \tilde{rv}_2)$ where $\tilde{rv}_{1,2}$ are independently drawn from Normal$(0, \alpha)$ and $\beta = 0.001$. Steady states for populations with increasingly asymmetric values ($\alpha \to 0.1$) for vital rates $r_{\max}$ and β are shown in warmer tones.

Figure S14: Near collapse of both populations with a low straying rate $m = 0.1$ and low trait heritability $h^2 = 0.2$ (see figure 4a). Black line marks the calculated point of recovery post-perturbation. Trait optima are $\theta_1 = 10$ (blue population trajectory) and $\theta_2 = 5$ (red population).